Ecotoxicology and Environmental Safety 257 (2023) 114932

Contents lists available at ScienceDirect

Ecotoxicology and Environmental Safety

journal homepage: www.elsevier.com/locate/ecoenv

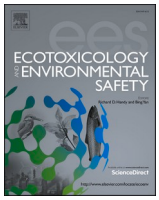

The importance of presoaking to improve the efficiency of $MgCl_2$-modified and non-modified biochar in the adsorption of cadmium

Bahram Abolfazli Behrooz [a], Shahin Oustan [b], Hossein Mirseyed Hosseini [a], Hassan Etesami [a,*], Elio Padoan [c], Giuliana Magnacca [d], Franco Ajmone Marsan [c]

[a] Department of Soil Science, College of Agriculture and Natural Resources, University of Tehran, Tehran, Iran
[b] Soil Science Department, Agricultural Faculty, University of Tabriz, Iran
[c] Dipartimento di Scienze Agrarie, Forestali e Alimentari, Università degli Studi di Torino, Grugliasco, TO, Italy
[d] Dipartimento di chimica, Università degli Studi di Torino, Torino, Italy

ARTICLE INFO

Edited by Dr Muhammad Zia-ur-Rehman

Keywords:
Presoaking mechanism
Adsorption kinetics
Cadmium removal
Mg-modified biochar

ABSTRACT

Investigating the effect of presoaking, as one of the most important physical factors affecting the adsorption behavior of biochar, on the adsorption of heavy metals by modified or non-modified biochar and presoaking mechanism is still an open issue. In this study, the water presoaking effect on the kinetics of cadmium (Cd) adsorption by rice husk biochar (produced at 450 °C, B1, and at 600 °C, B2) and the rice husk biochar modified with magnesium chloride (B1 modified with $MgCl_2$, MB1, and B2 modified with $MgCl_2$, MB2) was investigated. Furthermore, the effect of pH (2, 5, and 6), temperature (15, 25, and 35 °C), and biochar particle size (100 and 500 μm) on the kinetics of Cd adsorption was also investigated. Results revealed that the content of Cd adsorbed by the presoaked biochar was significantly higher than that by the non-presoaked biochar. The highest Cd adsorption capacity of MB2 and MB1 was 98.4 and 97.6 mg g^{-1}, respectively, which was much better than that of B1 (7.6 mg g^{-1}) and B2 (7.5 mg g^{-1}). The modeling of kinetics results showed that in all cases pseudo-second-order model was well-fitted (R^2>0.99) with Cd adsorption data. The results also indicated that the highest Cd adsorption values were observed at pH 6 in presoaked MB1 with size of 100 μm as well as at the temperature of 35 °C in presoaked MB2, indicating the optimum conditions for this process. The presoaking process was not affected by biochar size and pH, and the difference in adsorbed Cd content between presoaked biochars and non-presoaked ones was also similar. However, the temperature had a negative effect on presoaking. The presoaking process decreased micropores (<10 μm) in the biochars but had no effect on biochar hydrophobicity. Therefore, presoaking, which could significantly increase Cd adsorption and reduce equilibrium time by reducing the micropores of biochars, is suggested as an effective strategy for improving the efficiency of modified biochars or non-modified ones in the adsorption of contaminants (Cd) from aquatic media.

1. Introduction

With the rapid development of industrial activities, a large amount of wastewater containing heavy metals is discharged to environment, which has resulted in a number of serious health problems (Joseph et al., 2019; Kumar et al., 2021). The presence of cadmium, Cd(II), in aquatic ecosystems has become an important environmental concern worldwide. Due to its non-degradable properties and tendency for bioaccumulation in the food chain, Cd poses a severe threat to the entire ecosystem (Khan et al., 2020). Therefore, developing a promising and effective technology to remove Cd from aqueous solution is of great significance for water safety and public health. Several methods (e.g., adsorption, chemical precipitation methods, advanced oxidation, electrochemical methods, and bioaccumulation) have been successfully applied to treat heavy metals including Cd (Deng et al., 2021; Khan et al., 2020; Zhang et al., 2021). Among them, the adsorption is an important clean technology in the treatment process (Yadav et al., 2021).

Adsorbents such as carbon nanomaterials, activated carbon, graphene materials, and biosorbents have been adopted to remove metals from aqueous environments (Agarwal and Singh, 2017), but these materials have high costs and complicated operations (Chen et al., 2018).

* Corresponding author.
E-mail address: hassanetesami@ut.ac.ir (H. Etesami).

https://doi.org/10.1016/j.ecoenv.2023.114932
Received 9 February 2023; Received in revised form 14 April 2023; Accepted 16 April 2023
0147-6513/© 2023 The Author(s). Published by Elsevier Inc. This is an open access article under the CC BY-NC-ND license (http://creativecommons.org/licenses/by-nc-nd/4.0/).

Biochar as a new efficient and inexpensive material has been widely applied for the remediation of environmental pollutants (Lucaci et al., 2019). It is prepared by pyrolysis and carbonization of agricultural wastes under limited oxygen or anaerobic conditions (Wang et al., 2019), and thus has the advantages such as rich functional groups, high exchangeable cation, large specific surface area, and porous structure (Agarwal and Singh, 2017; Qiu et al., 2021). Due to abundant feedstocks and simple preparation method, biochar has been regarded as an effective adsorbent with acceptable low cost and is widely applied to remove heavy metals from various environments (Jiang et al., 2012; Qiu et al., 2021). However, pristine biochar has usually a limited capacity to adsorb contaminants from aqueous solutions due to the low surface area compared with activated carbon (Tan et al., 2016). Therefore, biochar modification is necessary to increase the metal adsorption capacity. The modification methods include chemical modification, physical modification, loading with mineral oxides, and magnetic modification (Naeem et al., 2019; Nnadozie and Ajibade, 2020; Rajapaksha et al., 2016). Compared with pristine biochars, the metal-modified biochars can significantly enhance the properties of functional groups (–COOH, –OH, and –C═O), surface specific areas, pore structures, and cation exchange capacity (CEC) (Ding et al., 2016; Wang et al., 2019), and thus can provide more adsorption sites for heavy metals (Ding et al., 2016). Recently, magnesium (Mg)-modified biochars have received more attention due to their low toxicity and high adsorption capacity for the removal of heavy metals from aquatic media (Creamer et al., 2018; Deng et al., 2021; Wu et al., 2021; Yin et al., 2021). Mg-modified biochars are mainly coated with the particles of MgO and $Mg(OH)_2$, which are different products produced under different pyrolysis conditions (Creamer et al., 2018).

Biochar characteristics are affected by biochar production conditions and feedstock type (Kloss et al., 2012). For example, an increase at pyrolysis temperature causes a decrease in aliphatic chains of matrix and CEC and an increase in the specific surface area and aromatic moieties of the biochar (Kloss et al., 2012). The change of raw materials also makes the prepared biochar have different physicochemical properties, thus affecting the efficiency of biochar (Arán et al., 2016; Zhang et al., 2021). In addition, the experimental conditions also have an important role in determining the efficiency of biochar in metal adsorption (Berslin et al., 2021). Several scientists investigated the effect of pH, ionic strength and ionic competition for the removal of heavy metals from aqueous media to achieve the best conditions for a highly efficient process. In a study conducted on the removal of Cd from an aqueous solution, the maximum amount of Cd adsorption was observed at pH 7, and the decrease in the ionic strength of the solution limited the interaction of the ions in the solution (Park et al., 2017). Similarly, in another study (Xiao et al., 2017), the highest amount of Cd adsorption was reported at slightly acidic pH and low ionic strength. According to these researchers, the electrostatic repulsion between the adsorbent material and the adsorbate material is reduced and the proton competition is also limited.

Physical separation of biochar particles from aqueous solutions is always known as one of the most important challenges in the application of biochar in aqueous environments (Huang et al., 2021). Magnetization has been proposed as an efficient method to solve this problem, such as functionalizing rice straw biochar with iron compounds (Huang et al., 2021). Although all biochar production conditions are necessary to achieve good results in water decontamination applications, another important factor to consider is the possibility of improving the physical contact of biochar with aqueous solutions. In fact, the adsorption of ions on biochar requires intimate contact of the solid phase with the liquid phase (Brown et al., 2018). Since biochar is a porous and partially hydrophobic material (Gray et al., 2014), both the external and internal surfaces of biochar are required to achieve the best metal adsorption conditions. In addition, the surface character of an absorbent can affect the rate of adsorption, and the equilibrium of the adsorption process can occur in a shorter time with suitable affinity (Brown et al., 2018), allowing to reduce process time.

It seems that water presoaking is one of the most important physical factors in adsorption, which can affect the absorption behavior of adsorbents by improving the physical properties of adsorbents such as surface area, pore distribution, hydrophobicity, and creation of pores (Gao et al., 2019; Zhai et al., 2020). For example, Ai et al. (2021), by investigating the effect of water soaking on the mechanical properties and structure of coal, found that water soaking changes pore structure, surface properties, and pore connectivity of the coal. In a similar study, Soedarmanto et al. (2020) reported that water soaking after pyrolyzing changed the surface area and pore structure of activated carbon. In another study (Yi et al., 2022), soaking coal in water also increased pore number, pore size, and pore development. Also, the surface activity of coal and the content of functional groups such as aromatic ether, hydroxyl and methylene groups were affected by water soaking (Yi et al., 2022). These studies show that presoaking can improve the physical contact of adsorbent with adsorbate. Therefore, presoaking seems to be an effective way to enhance adsorption capacity of biochar. Despite the importance of presoaking in the adsorption process, little attention has been paid to the effect of presoaking on metal adsorption kinetics in modified or unmodified biochars. In addition, the mechanism of presoaking in changing the behavior of biochar is not clear. Accordingly, this study was conducted to investigate: (*i*) the effect of biochar presoaking on Cd adsorption kinetics in $MgCl_2$-modified and unmodified rice husk biochars; and (*ii*) the effect of pH, particle size of biochar, and temperature on the presoaking process.

2. Materials and methods

2.1. Biochar production and its modification

Rice husks, as main agricultural wastes in north of Iran, were used as feedstocks. The feedstocks were obtained from Astana rice processing factory (Gillan province, Iran), passed through a 10-mesh sieve, and dried at 70 °C for 24 h. To produce $MgCl_2$-modified biochar (MB), 2.5 L of 1 M $MgCl_2$ solution was added to 500 g rice husk, and stirred for 24 h and dried at 70 °C for 48 h. The $MgCl_2$ non-treated or treated rice husks were then heated in a muffle oven at 450 °C (Biochar 450 °C, B1) or at 600 °C (Biochar 600 °C, B2) under oxygen-free conditions under argon flow (10 $cm^3\ min^{-1}$) for 2 h. After cooling, the biochars were washed 10 times with distilled water to remove residual basic cations, and after each step, the electrical conductivity (EC) was measured to reach an EC value of < 1.5 dS m^{-1}. Finally, modified and unmodified biochars were dried and passed through a 500-μm sieve and kept in closed containers for further experiments. To study the effect of biochar particle size on Cd adsorption, an aliquot of the biochars (Table S1) was ground to 100 μm before the experiment.

2.2. Biochar characterization

For pH and EC analysis, 5 g of biochar was suspended in 50 mL of deionized water and shaken at 120 rpm for 24 h. After shaking, the pH of the suspensions was measured immediately, whereas EC was measured after 20 min without further shaking. To determine ash content, the samples were dried at 105 °C and weighed, then heated for 6 h in a muffle oven at 750 °C in the presence of air. Finally, the weight of residues was measured, and the percentage of ash was determined from the following Eq. 1 (Singh et al., 2017).

$$\%\mathrm{Ash} = \frac{\mathrm{weight}_{\text{ residue after 750 °C}}}{\mathrm{weight}_{\text{150 °C dried}}} \times 100 \quad (1)$$

Total Cd content in the biochar samples was determined using the method reported in a previous study (Singh et al., 2017). Briefly, 0.2 g of biochar was placed in a digestion tube. Then, the samples were heated at 650 °C for 8 h. After cooling, 4 mL of HNO_3 was added to the samples and heated at 120 °C for 2 h, afterwards 4 mL of H_2O_2 and 1 mL of HNO_3 were added to tubes and heated at 80 °C for 2 h. After digestion, 6 M HCl

was added to tubes and kept at room temperature for 24 h. Finally, the samples were filtered (Whatman No. 41) and the concentration of the element was measured using ICP-MS (PerkinElmer NexION® 350D). Pore volume and surface area of biochar samples were measured by N_2 adsorption-desorption gas-volumetric analysis at nitrogen boiling point (Micromeritics ASAP 2020 Plus). The pH of the point of zero charge (pH_{pzc}) was measured according to a previous study (Faria et al., 2004). In brief, 0.15 g biochar was added to closed 100 mL Erlenmeyer flasks containing 50 mL 0 f 0.01 M $NaNO_3$ with pH adjusted between 2 and 12. Fourier transform infrared (FTIR) was used to determine the functional groups using a Vector 22 by Bruker, equipped with Globar lamp and DTGS detector and by considering 128 scans with a resolution of 4 cm^{-1} in the range of 400–4000 cm^{-1}. The total content of carbon, nitrogen, sulfur, and hydrogen in the biochar samples was determined using an elemental analyzer (Elementar UNICUBE). The oxygen content was determined from the difference of the total mass of carbon, nitrogen, sulfur, hydrogen and ash from the total mass of biochar. The physical properties and morphology of the surface of biochars were evaluated using scanning electron microscopy (SEM-EDX) with a ZEISS EVO 50 XVP with LaB_6 source, equipped with detectors for secondary electrons collection and an Energy Dispersive X-ray Spectrometry (EDS) probe for elemental analyses. The samples were covered with a chromium layer thickness of ~5 nm (Emitech K575X sputter coater equipped with a film thickness monitor and Cr target) before the analysis to prevent any charge.

2.3. Biochar presoaking and its evaluation

After washing, the biochars were dried for 24 h at 7 °C and cooled in a desiccator. Then, 10 mL of distilled water was added to the centrifuge tubes containing 0.5 and 0.2 g of unmodified and modified biochars, respectively. The biochars were completely immersed in water for the set time (0.5, 1, 2, 4, 8, 16, 24, and 48 h).

The hydrophobicity of the biochars was determined by using the method of ethanol drop penetration. The biochars were presoaked for 16 h with distilled water at 25 °C, and then air-dried. The presoaked or non-presoaked biochar (10 g) was placed in a plate (3 cm depth × 5 cm diameter) and a droplet of ethanol solution (0.2,0.04, 0.8, 1, 2, and 3.5 M) was added to the surface of the biochars. Finally, drop penetration time was measured and the biochars were classified according to a previous method (Kinney et al., 2012). In this method, the samples were classified based on the lowest ethanol concentration that the droplet penetrated (<10 s). The samples were classified as hydrophilic (<1 M), hydrophobic (1–2 M), strongly hydrophobic (2–3.5 M), and extremely hydrophobic (>3.5 M).

A water adsorption test was also conducted to evaluate the effect of presoaking on the pores of biochars. The biochars were presoaked for 16 h with distilled water at 25 °C, and then air-dried. The presoaked or non-presoaked air-dried biochar (2 g) was placed in 20 mL tubes, then transported into an isolated compartment and maintained for 10 days in equilibrium with a vapor pressure of KCl solutions (with osmotic pressures 20 and 30 bar). These solutions were prepared according to Van't Hoff's Eq. 2 (Van't, 1888). Finally, the moisture content of the biochar and the difference in adsorbed water between the presoaked or non-presoaked biochar were calculated:

$$\Pi = -iMRT \tag{2}$$

Where Π, R, T, M, and i are osmotic pressure (bar), the universal gas constant, absolute temperature (K), molar concentration, and Van't Hoff's factor of solute, respectively.

By using Eq. 3, the average pore diameter of the biochars at the osmotic pressures equivalent to 20 and 30 bar was calculated:

$$D = \frac{0.3}{h} \tag{3}$$

Where, D (cm) and h are biochar pore diameter and matric potential (cm), respectively (Jabro and Stevens, 2022).

2.4. Adsorption experiments

The kinetics experiments were conducted on (P) presoaked or (NP) non-presoaked adsorbents (biochars) in three replicates. During the presoaking process, 10 mL distilled water was added to centrifuge tubes containing 0.5 or 0.2 g of non-modified or modified biochars, respectively, and left in contact for 0.5, 1, 2, 4, 8, 16, 24, and 48 h. At the next step, 10 mL of Cd solution at pH 6 (400 mg L^{-1} of Cd for non-modified biochar and 2000 mg L^{-1} for modified biochar) was added to presoaked biochars at the prior step, and the samples were shaken at room temperature (25 ± 1 °C) for 0.5, 1, 2, 4, 8, 16, 24, and 48 h.

To study the kinetics of Cd adsorption by non-presoaked biochars, 0.5 or 0.2 g of the unmodified or modified biochar was placed in centrifuge tubes containing 20 mL of Cd solution (200 mg L^{-1} of Cd for unmodified biochar experiment and 1000 mg L^{-1} for modified biochar experiment) and the samples were shaken at 25 ± 1 °C for 0.5, 1, 2, 4, 8, 16, 24, and 48 h.

To investigate the effect of temperature and pH on Cd adsorption kinetics in non-modified biochars, the suspension pH was adjusted to 2, 5, and 6 and shaken at 15 ± 1 °C, 25 ± 1 °C, and 35 ± 1 °C, respectively, for previously mentioned contact time intervals. After each contact time, presoaked and non-presoaked biochar samples were centrifuged at 4000 rpm and filtered (Whatman No. 41) and the residual concentration of Cd in the solution was determined by ICP-MS. The adsorbed Cd was calculated from the difference between the initial concentration and the equilibrium concentration. Finally, Eq. 4 (pseudo-first order) (Lagergren S, K, 1898), Eq. 5 (pseudo-second order) (Ho and McKay, 1999), and Eq. 6 (intraparticle diffusion) (Weber, Morris, 1963) were used to model Cd adsorption kinetics:

$$log(q_e - q_t) = \log q_e - \frac{k_1}{2.0303}t \tag{4}$$

$$\frac{t}{q_t} = \frac{1}{k_2 q_e^2} - \frac{t}{q_e} \tag{5}$$

$$q_t = k_d t^{\frac{1}{2}} + c \tag{6}$$

Where q_e, c, and q_t are the amount of Cd (mg g^{-1}) adsorbed, respectively, at the equilibrium, at time zero, and at time t (h), and k_1, k_2, and k_d are the constant rate of pseudo-first-order (h^{-1}), pseudo-second-order (g m^{-1} g^{-1} h^{-1}), and intraparticle diffusion (mg g^{-1} $h^{-0.5}$), respectively.

2.5. Statistical analysis of data

After confirming the normality of the data by Kolmogorov–Smirnov test, the experimental data were analyzed using the SAS v.9.1 (SAS Institute Inc., Cary, NC). Reported data are the average of three replicates. To estimate the significant differences among some experimental treatments, Duncan's multiple range test ($p \leq 0.05$) was applied.

3. Results and discussion

3.1. Biochar characterization

The main properties of the biochars are reported in Table 1. With increasing pyrolysis temperature, the carbon content increased and the percentage of oxygen and H, and the atomic ratio of H to C and O to C decreased, indicating that the loss of hydrogen and oxygen from the matrix increases during the pyrolysis temperature (Angın, 2013; Zhang et al., 2015). It can also be observed that Mg was successfully loaded onto modified biochars and their element compositions and pore structures changed (Table 1). The ash content, EC, pH, %O, %H, and the

Table 1
Properties of modified and non-modified rice husk biochars.

Parameter	B1	B2	BM1	BM2
C (%)	50.5	53.5	41.2	38.0
H (%)	2.8	1.7	3.8	2.7
O (%)	16.2	12.1	20.6	18.4
N (%)	0.68	0.49	0.63	0.49
S (%)	0.024	0.018	0.022	0.019
H/C	0.056	0.032	0.093	0.071
O/C	0.32	0.27	0.49	0.48
pH (1:10)	7.4	7.7	8.2	8.6
EC ($\mu S\ m^{-1}$)	387	273	1215	1405
pH_{zpc}	5.8	6.0	8.5	9
BET Surface area ($m^2\ g^{-1}$)	28	195	66	231
Micropore volume ($cm^3\ g^{-1}$)	0.011	0.085	0.017	0.081
Ash (%)	30	32.98	33.8	40.4
Total Cd ($mg\ kg^{-1}$)	0.05	0.05	0.06	0.07

B1, rice husk biochar produced at 450 °C; B2, rice husk biochar produced at 600 °C, MB1, husk biochar produced at 450 °C and modified with $MgCl_2$; and MB2, husk biochar produced at 600 °C and modified with $MgCl_2$.

atomic ratio of H to C and O to C of the biochars increased after modification. However, the carbon content of the biochars decreased after modification. Similar trend was found in a previous study (Deng et al., 2021). The increase in ash content, EC and pH can be attributed to the adsorption and precipitation of magnesium on the surface of biochar after biochar modification. Also, the ratio of oxygen and hydrogen in modified biochar was significantly higher than that of unmodified biochar, indicating that Mg-modified biochars help to maintain H and O content and increase oxygen functional groups, as well as increase the hydrophilicity of Mg-modified biochars (Creamer et al., 2018; Xu et al., 2017), all of which are favorable to heavy metal adsorption. FTIR analysis (Fig. 1) also confirms that the increase in oxygen and hydrogen content is due to the formation of hydroxyl and carboxyl functional groups in the modified biochars.

The pH_{zpc} results (Table 1) showed that the pH_{zpc} values in B1 and B2 were in the acidic range ($pH_{zpc} < 7$), while the pH_{zpc} values in MB1 and MB2 were in the basic range ($pH_{zpc} > 8.5$), indicating that Mg-modified biochars contain more alkaline functional groups (such as hydroxyl and phenol) and can be favorable for heavy metal adsorption. Similar trend was also found in the previous studies (Deng et al., 2021; Nguyen et al., 2022; Sun et al., 2019).

The results of the surface area and pore volume analysis of the biochars demonstrated that the surface area and volume of the micropores

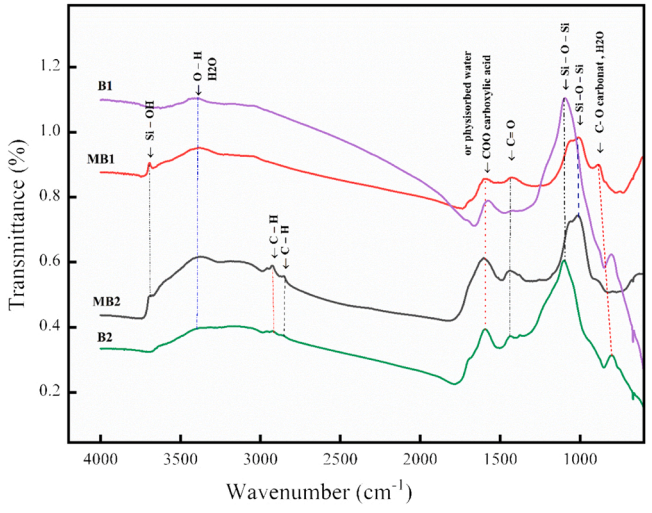

Fig. 1. : FTIR analysis of non-modified biochars (B1 and B2) and modified biochars (MB1, and MB2). The spectra were shifted to facilitate the observation of the curves.

increased with increasing the pyrolysis temperature (Table 1). With increasing the pyrolysis temperature from 450 to 600°C, surface area increased by 235% and 119% in unmodified biochars and modified biochars, respectively. Similar results were also reported in a previous study (Shen et al., 2019). The increase in pyrolysis temperature causes the creation of channels, the degradation of lignin and hemicelluloses and the release of CH_4 and H_2 (volatile gases), which greatly increases the surface area (Zhang et al., 2015). Also, the surface area of the biochars increased from 28 to 66 $m^2\ g^{-1}$ and from 195 to 231 $m^2\ g^{-1}$ after modification at temperature of 450 and 600 °C, respectively (Table 1). Shi et al. (2019) also reported similar results on rice husk biochar. These authors showed an increase in biochar surface area from 0.63 to 193.1 $m^2\ g^{-1}$ following an increase in pyrolysis temperature from 300 to 700°C. They also reported that modification has a significant effect on the biochar surface area. In the study of Chen et al. (2014), biochar modification also caused an increase in the specific surface area from 25.4 to 67.6 $m^2\ g^{-1}$. In the present study, with enhancing pyrolysis temperature from 450 to 600°C, the volume of the micropores increased from 0.011 to 0.085 $cm^3\ g^{-1}$ and from 0.017 to 0.081 $cm^3\ g^{-1}$ in unmodified biochar and modified biochar, respectively. This confirms that only a small effect of $MgCl_2$ modification on the microporosity of the systems is visible while increasing pyrolysis temperature could enhance the volume of the micropores 7–8 times. This increase in the volume of the micropores during pyrolysis can be attributed to the rupture of cellulose and hemicellulose (Chatterjee et al., 2020). In the study of Deng et al. (2021), the pore structure properties of biochar were improved by modification, and the specific surface area for Mg-modified biochar increased from 12.68 (non-modified biochar) to 52.41–174.29 $m^2\ g^{-1}$. These researchers attributed this increase in the surface area and pore volumes of modified biochars to the improvement of the pore structure when the biochar was impregnated with magnesium oxide particles.

FTIR analysis of modified or non-modified biochars is shown in Fig. 1. An intense and large signal related to the stretching of O-H groups interacting via H bonding was present in the spectra of all biochars at 3400 cm^{-1}, while a narrow signal centered at 3700 cm^{-1}, due to isolated Si-OH functional groups, was present only in the spectra of the modified biochars, indicating the effect of modification on increasing the number of OH groups and consequently the hydrophilicity of the biochars. The same result was also reported in a previous study (Quan et al., 2020). In another study, a new strong adsorption peak was observed in 3469 cm^{-1} in magnesium-modified corn biochar, which was attributed to Mg $(OH)_2$ formation at the surface of the biochar (Deng et al., 2021). In MB2, three peaks were clearly observed below 3000 cm^{-1}, indicating the presence of aliphatic carbon chains (stretching of C-H moieties). Additionally, carbonate-like groups, which are derived from atmospheric CO_2 interaction with the basic surface of biochars, and physisorbed water molecules were also evidenced in the spectra in the range of 1800–1200 cm^{-1}. Intense bands were present for carboxyl, ketone, C = C, and C = O groups at 1428, 1580 cm^{-1}, and 1099 cm^{-1}, respectively. Similar results were also reported in a previous study (Teng et al., 2020). Also, the Si-O-Si spectroscopic feature was observed at 1000 cm^{-1} in all biochars (Fig. 1), which was slightly shifted by modification procedure that can be attributed to the presence of inorganic silica in the rice husk (Usman et al., 2016; Xiao et al., 2017). In all cases, the modification appears to have introduced polar oxygen-containing functionalities to the biochar surface.

SEM images showed structures similar to plant tissues at the B1 and B2 surfaces (Fig. 2). With increasing pyrolysis temperature from 450 to 600°C, the irregularity of surfaces increased and some macroporosity in the structure was created. Biochar modification also increased the irregularity and porosity of the structures, as the MB1 and MB2 showed irregular shapes and rough surfaces. The surface morphology of MB1 biochar exhibited a smoother aspect than that of MB2. Also, the porosity and the extension of pores in MB2 were higher than those in MB1 (Fig. 2a and b).

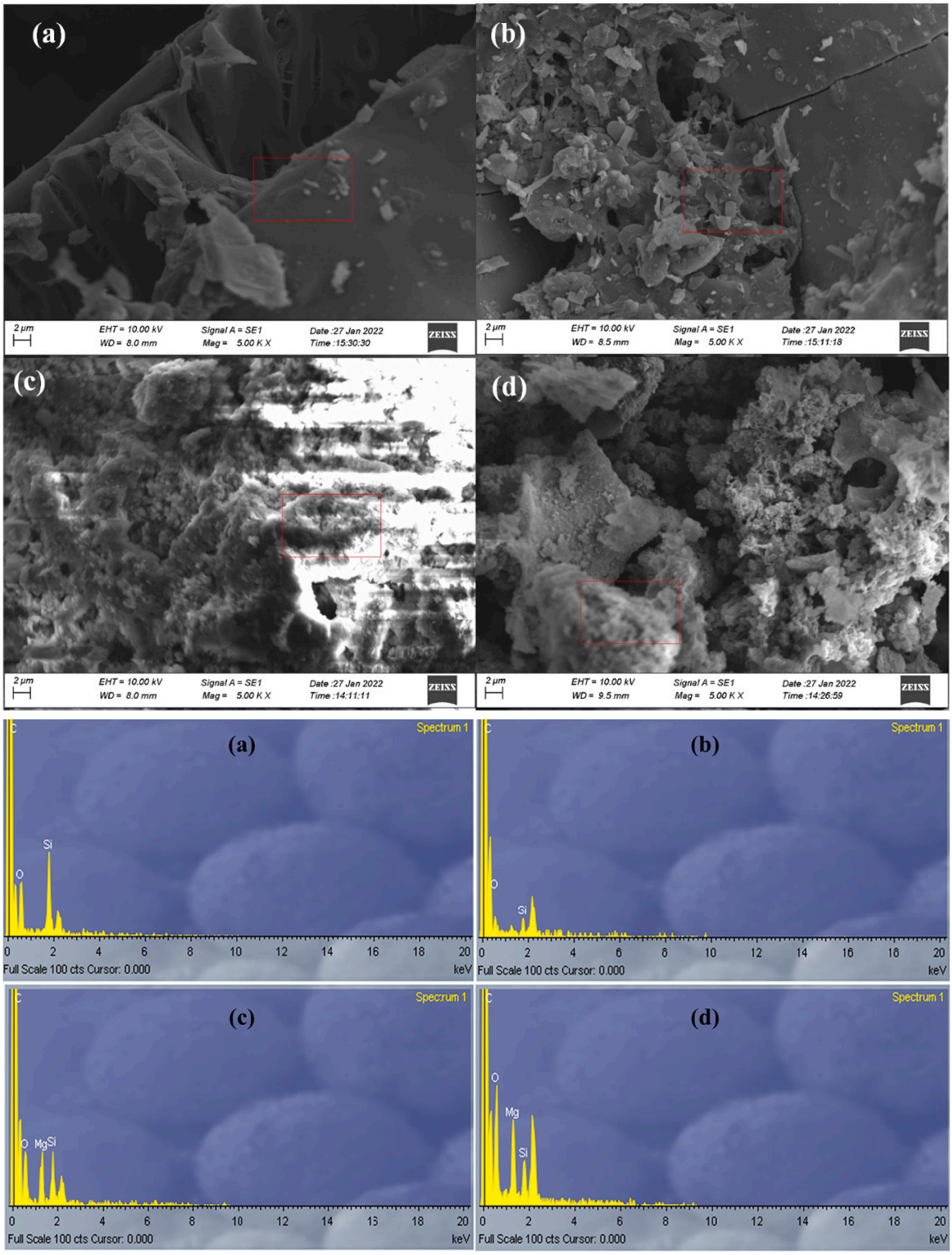

Fig. 2. : SEM-EDS images of (a), B1; (b), B2; (c), MB1; and (d), MB2. B1, biochar produced at 450 °C; B2, biochar produced at 600 °C, MB1, biochar produced at 450 °C and modified with $MgCl_2$; and MB2, biochar produced at 600 °C and modified with $MgCl_2$.

The results of the EDS analysis confirmed the presence of a high magnesium content (>12%) on biochars (Fig. 2). It was probably in the form of MgO, which was also confirmed in a previous study (Yin et al., 2021). The ratios of O to C calculated using the EDS results for the modified samples of MB1 and MB2 were 0.78 and 0.60, respectively, which are quite different and generally higher than the values obtained from the elemental analysis (0.48 and 0.49, respectively). The results also indicated an increase in oxygen content in the modified samples, as also observed by Akram et al. (2022), and confirm the FTIR results, which indicated the formation of oxygen-containing functionalities after biochar modification. Furthermore, since EDS analyzes the surface of the particles and reflects the information related to the surface, it can be concluded that the increase in oxygen content shown is related to the surface or the outermost layers of the biochar. According to the results mentioned above, Mg-modified biochars can provide more adsorption sites for heavy metal.

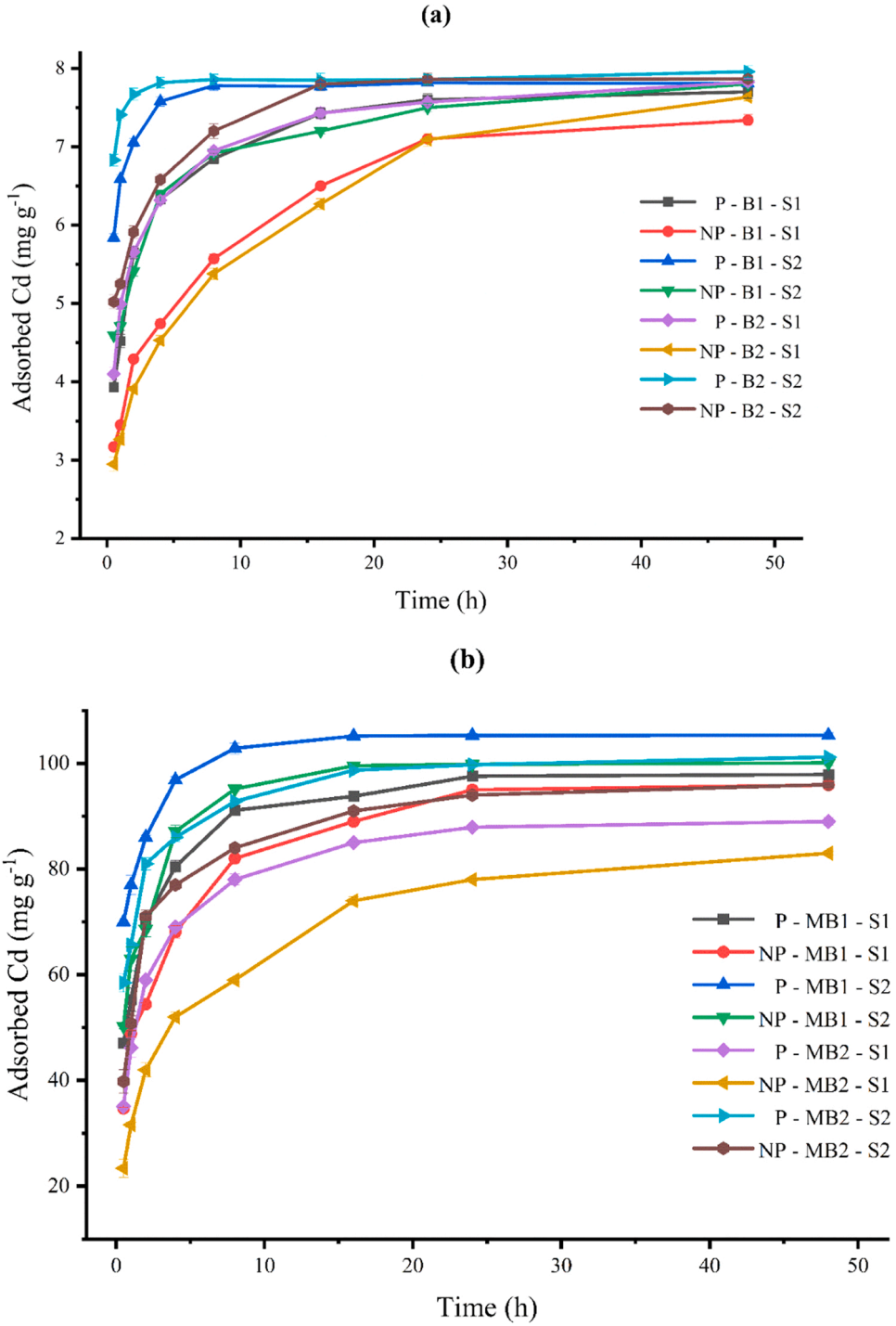

Fig. 3. : Effect of biochar size (500 μm, S1, and 100 μm, S2) on Cd adsorption kinetics in (a) unmodified biochars and (b) modified biochars. P, presoaked biochar; NP, non-presoaked biochar; B1, biochar produced at 450 °C; B2, biochar produced at 600 °C, MB1, biochar produced at 450 °C and modified with $MgCl_2$; and MB2, biochar produced at 600 °C and modified with $MgCl_2$.

3.2. Effect of experimental conditions on biochar presoaking process

3.2.1. Effect of biochar size

The effect of biochar size and biochar presoaking on Cd adsorption was investigated at 500 μm size (S1) and 100 μm size (S2). The results showed that, by reducing the biochar particle size from 500 to 100 μm in modified and unmodified biochars, the adsorption of Cd by these biochars increased significantly. However, biochar size reduction from 500 to 100 μm did not significantly change the Cd adsorption rate by presoaked and non-presoaked biochars. This shows that reducing biochar size does not have a remarkable effect on the presoaking process. According to Fig. 3, the presoaking process changed the distribution of micropores (diameter less than 10 μm) in the presoaked biochars. Grinding the biochar to reduce the size of the biochar will not probably change the micropore distribution. Also, the effect of presoaking on Cd adsorption was more evident than the size effect, as Cd adsorption in P-B1-S1 was close to that in NP-B1-S2 (Fig. 3). The effect of presoaking on Cd adsorption increased with increasing contact time from 0.5 to 6 h, and after 6 h this effect decreased. Therefore, the maximum effect of presoaking was determined between 4 and 6 h. Also, both biochar size reduction and biochar presoaking had a greater effect on Cd adsorption in modified biochars compared to unmodified biochars, which could explain the high Cd adsorption capacity of modified biochars. The optimal size of biochar for Cd removal in both presoaking and non-presoaking conditions was determined to be 100 μm.

The time to reach the equilibrium was reduced from 24 to 12 h (except for BM2) by presoaking and decreasing biochar size (Fig. 3). The increased Cd adsorption and reduced equilibrium time were presumably due to the creation of new pores and the increase of the specific surface area in smaller particles. Smaller particles are also more conductive and have higher densities of functional groups at the external pores (Jin et al., 2022), which can increase the biochar reactivity and the amount of Cd adsorption. Another possible mechanism for increasing the Cd adsorption by smaller particles is the formation of graphite-like structures and nanostructures (Song et al., 2019). Jin et al. (2022) also reported a positive correlation among biochar size, graphite structures and functional groups. Smaller particles had more graphite-like structures and functional groups (Jin et al., 2022). Therefore, the biochars with smaller particles were more active and had higher Cd adsorption rates than biochar with larger sizes. According to the above results, the reduction of biochar size mainly led to the increase of the specific surface area and the formation of graphite-like structures, which reduced the presoaking effect by increasing the physical contact. On the other hand, biochar size reduction led to the formation of new pores and nanostructures, which increased the effect of presoaking. Therefore, biochar size reduction, although it increased adsorption, did not affect the presoaking process.

3.2.2. Effect of temperature

The effect of presoaking on the Cd adsorption kinetics in non-modified biochars and modified ones at different temperatures is shown in Fig. 4. At all temperatures, Cd was adsorbed in presoaked biochars more than non-presoaked biochars and the effect of presoaking process on Cd adsorption decreased with increasing reaction temperature and contact time. The difference of adsorbed Cd by presoaked and non-presoaked biochars decreased with increasing temperature from 15° to 35°C, as this trend was more evident in B1 and BM1. In both unmodified and modified biochars, the highest Cd adsorption was observed in presoaked biochars at 35°C and the lowest Cd adsorption was observed in presoaked biochars at 15°C. Also, the greatest effect of presoaking on Cd adsorption was observed at the period of 6–8 h, and the difference of Cd adsorption between presoaked and non-soaked conditions decreased after 8 h, then it was minimized at 24 h. The amount of Cd adsorbed by modified biochars was higher than that by unmodified biochars at all temperatures. Also, the increase of Cd adsorption during the presoaking process was higher in modified biochars than in unmodified biochars, which was related to the high adsorption capacity of modified biochars. The time to reach equilibrium was reduced from 48 h at 15°C to 24 h at 35°C with presoaking and increasing temperature. Considering the presoaking temperature and time, the optimal adsorption of Cd by presoaked biochars was obtained at 35 °C. An increase in temperature is known to decrease the density of the suspension, which increases the rate of diffusion of solutes into the external and internal pores, which affects adsorption and reduces the time to reach equilibrium (Srivastava et al., 2007; Srivastava et al., 2006). On the other hand, it is known that the increase in temperature increases the hydraulic conductivity of biochar pores, which is explained by the decrease in water viscosity and the increase in pore volume (Saha and Tripathi, 1979; Yang et al., 2022). As a result, the transfer of Cd solution to biochar pores (especially micropores) is facilitated, and more internal surfaces will be in contact with Cd ions, and subsequently Cd adsorption increases. This could explain the decrease of the presoaking effect with increasing temperature in this study. In general, two driving forces are involved in the adsorption process; enthalpy (ΔH) and entropy (ΔS) of reaction (Brown et al., 2018). Previous studies reported that the enthalpy of the Cd adsorption process is small and positive, indicating that the adsorption is endothermic (Sheela and Nayaka, 2012). It has also been reported that the entropy of the Cd adsorption is positive due to the increase in randomness at the interface between particles and the solution (Wang et al., 2017). At the expense of ΔS and ΔH, the ΔG is a negative value. In a previous study, Xiang et al. (2018) measured ΔG values for the Cd adsorption at temperatures of 25, 35 and 45 °C, which were − 8612, − 8901, and 9.191 kJ mol^{-1}, respectively. Therefore, the Cd adsorption process is a non-spontaneous and endothermic reaction. Accordingly, as also shown in a previous study (Zhou et al., 2014), Cd adsorption should be increased with increasing temperature.

3.2.3. Effect of pH

In this study, the effect of biochar presoaking on Cd adsorption was examined at pHs 2, 5, and 6. According to this assay, the difference in Cd adsorbed by presoaked and non-presoaked biochars at different pHs was similar and the presoaking process was not affected by pH change. This confirms that the presoaking process is a physical modification. Also, the results of the water adsorption test confirmed the fact that the presoaking process was a physical reaction and was not affected by pH changes (Tables 2 and 3). As shown in Fig. 5, Cd adsorption increased dramatically as pH increased from 2 to 6. However, presoaking had a strong effect on Cd adsorption by B1, B2, MB1, and MB2. In addition, Cd adsorption by presoaked biochars at pH 3 and 5 was higher than that by non-presoaked biochar at pH 5 and 6. This shows that the effect of presoaking on Cd adsorption was greater than pH effect on Cd adsorption. At all contact time intervals, Cd adsorption was significantly higher in presoaked biochars than non-presoaked ones. At all pHs, the adsorption of Cd by modified biochars was higher than that by non-modified biochars and the lowest and highest adsorption of Cd were observed in MB2 and B1 at the same pHs (Fig. 5). This can explain the strong effect of presoaking on Cd adsorption by modified biochars. According to the results mentioned above, the maximum adsorption of Cd was observed in the presoaked status at pH 6. According to Wang et al. (2021), the significant increase in Cd adsorption as well as the increase in pH from 2 to 6 can be related to the decrease in the competition between protons and Cd ions on the biochar surface. According to previous studies, changes in pH also affect both the properties of the adsorbent and the properties of the adsorbate (Usman et al., 2016). The main effect of pH on the surface of biochar is protonation and deprotonation of functional groups such as carboxyls, hydroxyls, and phenols. Increasing pH increases Cd adsorption for deprotonation of functional groups, which increases negative charge density on biochar surfaces and reduces competition between protons and Cd ions on adsorption sites (Usman et al., 2016). On the other hand, pH is also an important parameter that affects ion speciation and consequently ion adsorption (Wen et al.,

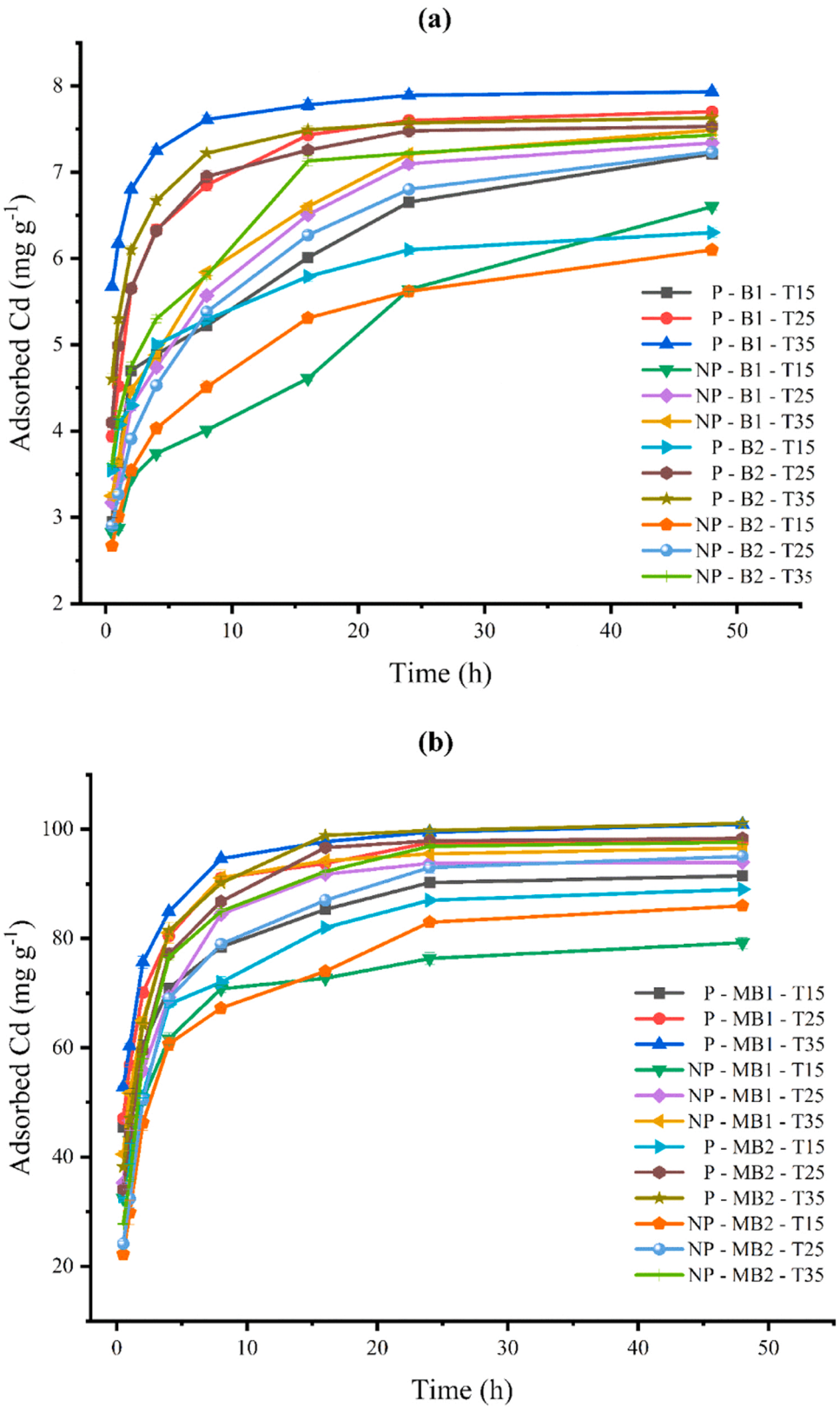

Fig. 4. : Effect of temperature on Cd adsorption kinetics in biochars. P, presoaked biochar; NP, non-presoaked biochar; B1, biochar produced at 450 °C; B2, biochar produced at 600 °C, MB1, biochar produced at 450 °C and modified with $MgCl_2$; and MB2, biochar produced at 600 °C and modified with $MgCl_2$. T15, T25, and T35 are temperature at the 15, 25, and 35 °C, respectively.

Table 2
Hydrophobicity property of non-modified and modified biochars.

Biochar Type	Presoaking	Molarity of ethanol drop (M)	Drop penetration time (s)	Category
B1	P	0.2	< 1	Hydrophilic
	NP	0.2	7.6	Hydrophilic
B2	P	0.2	< 1	Hydrophilic
	NP	0.2	5.2	Hydrophilic
MB1	P	0.2	< 1	Hydrophilic
	NP	0.2	4.1	Hydrophilic
MB2	P	0.2	< 1	Hydrophilic
	NP	0.2	2.9	Hydrophilic

P, presoaked biochar; NP, non-presoaked biochar; B1, biochar produced at 450 °C; B2, biochar produced at 600 °C, MB1, biochar produced at 450 °C and modified with $MgCl_2$; and MB2, biochar produced at 600 °C and modified with $MgCl_2$.

Table 3
Effect of different osmotic pressures on water content of non-modified and modified biochars.

Biochar Type	Presoaking	Water content (g or cm^3 water g^{-1} biochar)		Difference in adsorbed water between P and NP biochar (g or cm^3)	
		Osmotic pressure (bar)			
		20 bar	30 bar	20 bar	30 bar
B1	P	0.055	0.052	0.022	0.017
	NP	0.099	0.087		
B2	P	0.055	0.053	0.028	0.022
	NP	0.11	0.099		
MB1	P	0.092	0.086	0.026	0.019
	NP	0.121	0.11		
MB2	P	0. 13	0.12	0.026	0.017
	NP	0.27	0.236		

P, presoaked biochar; NP, non-presoaked biochar; B1, biochar produced at 450 °C; B2, biochar produced at 600 °C, MB1, biochar produced at 450 °C and modified with $MgCl_2$; and MB2, biochar produced at 600 °C and modified with $MgCl_2$.

2022). Wang et al. (2022) also observed that the adsorption of antibiotics on biochar decreases with decreasing pH due to the protonation of the functional groups and the creation of a positive charge.

3.3. Adsorption kinetics

The results of Cd adsorption kinetics on modified and unmodified biochars showed that rapid adsorption occurred in less than 1 h, followed by slower adsorption up to 24 and 48 h. Finally, the adsorption reactions in modified and unmodified biochars reached equilibrium after 24 and 48 h, respectively (Fig. 6). Similar results were also observed in a previous study (Xiao et al., 2017). At the rapid step, 43%, 48%, 49%, and 35% of Cd were adsorbed in non-presoaked B1, B2, BM1, and BM2, while in presoaked B1, B2, BM1, and BM2, 59.08%, 58.3%, 58.1%, and 45% of Cd adsorption occurred at this step. This indicates that presoaking improved the rate of Cd adsorption at the rapid step, which was confirmed by reduction of equilibrium time in presoaked treatments. It seems that the presoaking process improves the pore connectivity, the enlargement of pores, and the hydraulic conductivity of pores (Yi et al., 2022; Zhai et al., 2020). Following this process, a larger volume of Cd-containing solution entered the pores and more sites were available for cadmium adsorption, and accordingly, the rate of cadmium adsorption increased in the fast phase. As shown in Fig. 6, the effect of presoaking on Cd adsorption first increased with increasing contact time, and the maximum effect of presoaking was observed between 4 and 6 h. It decreased after 6 h and reached a minimum when the adsorption reaction reached equilibrium. It seems that in the early days, all the pores were not yet filled with water, and after 4–6 h, most of the biochar pores were saturated with water and the maximum effect of presoaking was observed. After 6 h, almost all the pores were saturated with water and the difference of Cd adsorbed between pre-soaked and non-soaked biochar decreased. Similar results were also reported in a previous study (Ai et al., 2021).

The values of Cd adsorption in the equilibrium status for B1, B2, MB1 and MB2 were 7.6, 7.5, 97.6 and 98.4 mg g^{-1}, respectively, and for non-presoaked B1, B2, MB1 and MB2 were 7.33, 7.14, 93.9 and 95 mg g^{-1}, respectively. The highest and lowest adsorbed Cd were observed in presoaked MB2 and non-presoaked B2 (Fig. S1 and S2). Cadmium adsorption in presoaked biochars was significantly higher ($p < 0.05$) than that in non-presoaked ones (Fig. S1 and S2). This could be due to more effective adsorbate/adsorbent contact in presoaked biochars, where the hydrophobicity of the samples is at least partially reduced (Gray et al., 2014). Also, the effect of presoaking on Cd adsorption was more evident in modified biochars (MB1 and MB2) than unmodified biochars (B1 and B2). This can be attributed to the high adsorption capacity in modified biochars compared to unmodified biochars.

Pseudo-first order, pseudo-second order, and intraparticle diffusion models were used to model Cd adsorption kinetics (Table 4). Among these three models, the pseudo-second order model showed the highest correlation coefficient ($R^2 > 0.99$) and well simulated the results of the Cd adsorption process in modified and non-modified biochars. Li et al. (2017) also found that the sorption kinetics of Cd(II) on BC-MnO_x follows a pseudo-second-order model, and the main mechanisms involve cation exchange and cation-Π bonding. In another study, Ifthikar et al. (2017) reported that magnetic biochar adsorbed Pb(II), which is well-described by a pseudo-second-order model; the adsorption mechanisms involve electrostatic attraction, ion exchange, complexation and precipitates. The adsorption equilibrium values obtained from the pseudo-second-order model were very close to the experimental results, and indicated that chemisorption in the form of cation exchange, precipitation, and inner sphere complexes is probably the main process controlling Cd adsorption in the biochars (Usman et al., 2016). Liu and Fan (2018) also pointed out that the precipitation with minerals is the main process in the removal of Cd by wheat straw biochar, and surface complex process plays an important role in this regard. Also, the pseudo-first order model was well fitted ($R^2 > 0.91$) with the kinetics data, which shows that mass transfer is also one of the important processes in Cd adsorption on the biochar surface. The intraparticle diffusion model compared with pseudo-first order and pseudo-second order model was not well fitted with Cd adsorption data, which indicates that the intra-particle diffusion or film diffusion is not a rate-limiting step in Cd adsorption by the biochars. Therefore, intra-particle diffusion has a lesser role than chemisorption. Accordingly, it can be concluded that chemisorption and mass transfer are the important factors controlling Cd adsorption process (Fulazzaky, 2011; Gao et al., 2019; Khan et al., 2020; Kołodyńska et al., 2012).

3.4. Action mechanism of presoaking process

Hydrophobicity experiment was performed in the range from 0.2 to 3.5 M ethanol solution. According to the classification of Kinney et al. (2012), all biochars were classified in the hydrophilic group (Table 2). Also, there was little difference between presoaked biochars and non-presoaked ones in terms of drop penetration time. Although both presoaked biochars and non-presoaked ones were classified in the hydrophilic group, biochar micropores might be hydrophobic. Similar results were also reported in a previous study (Rasa et al., 2018).

Water adsorption test was carried out to explain what happened in pores during biochar presoaking. According to Table 3, the water content in the matric potential 20 and 30 times was higher in non-presoaked biochars biochar than in presoaked biochars. The average pore diameter at the osmotic pressures equivalent to 20 and 30 bar was calculated to be 15 and 10 μm, respectively. In addition, the water content at 30 bar osmotic pressure was higher in non-presoaked biochars than presoaked biochars, indicating that the micropores of the biochar (< 10 μm) in

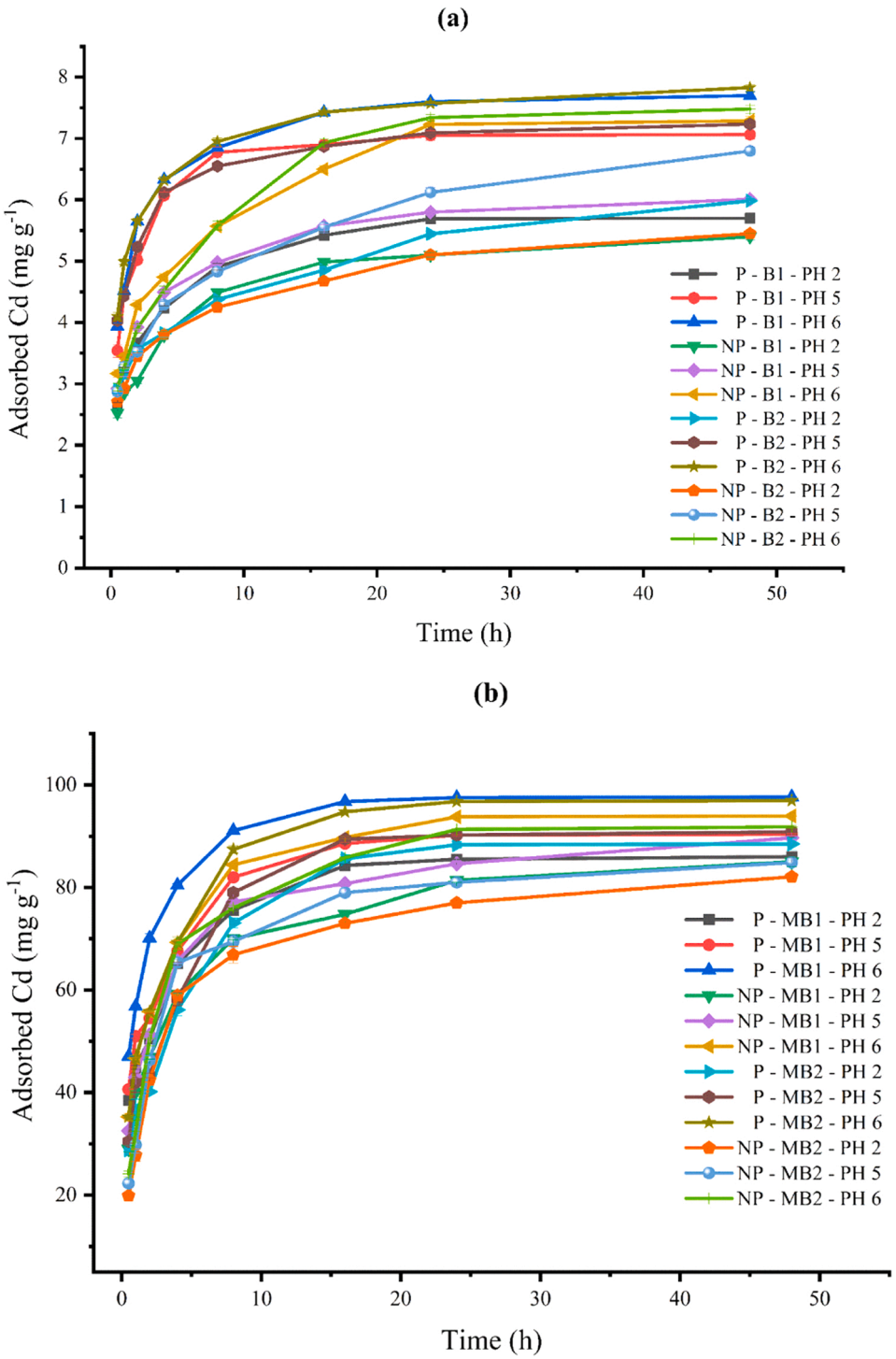

Fig. 5. : Effect of pH on Cd adsorption kinetics in biochars P, presoaked biochar; NP, non-presoaked biochar; B1, biochar produced at 450 °C; B2, biochar produced at 600 °C, MB1, biochar produced at 450 °C and modified with $MgCl_2$; and MB2, biochar produced at 600 °C and modified with $MgCl_2$. pH 2, pH 5, and pH 6 are pH at the 2, 5, and 6, respectively.

non-presoaked biochars were more than those in presoaked biochars, and consequently micropores were reduced by presoaking. The reduction of micropores can be attributed to the micropores that have been destroyed or even turned into macropores due to the change in tar distribution and the swelling phenomenon during presoaking (Rasa et al., 2018), which causes the reduction of micropores in non-presoaked biochars and confirms the reason. In addition, throat size, as an important factor in pore hydraulic behavior, was affected by changes in pore size, which can impact the rate of diffusion in micropores. Ai et al. (2021) also reported that soaking coal in water changes the pore structure and turns micropores into macropores. Rasa et al. (2018) announced that the ratio of throat size to pore size decreases with decreasing pore size and there is an inverse relationship between throat effect and pore size. According to the obtained results, the main mechanism of presoaking was found to be the change in the micropore size. It is known that the pore scale, solute transport and hydraulic properties of porous media are controlled by pore size distribution and pore topology (Ai et al., 2021; Nimmo, 2004; Vogel and Roth, 2001). Based on the

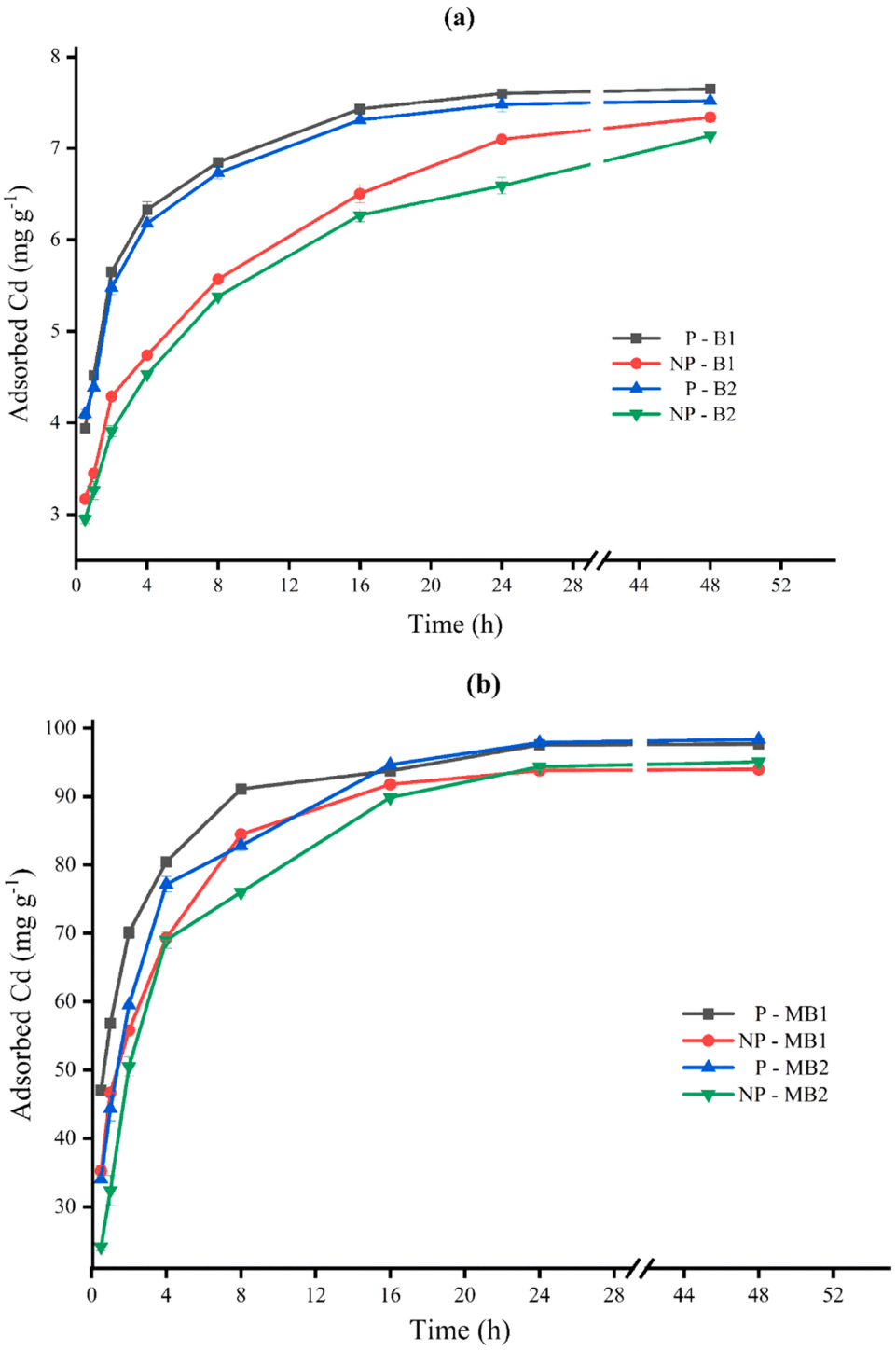

Fig. 6. : Adsorption kinetics of Cd in (a) unmodified biochars and (b) modified biochars. P, presoaked biochar; NP, non-presoaked biochar; B1, biochar produced at 450 °C; B2, biochar produced at 600 °C, MB1, biochar produced at 450 °C and modified with $MgCl_2$; and MB2, biochar produced at 600 °C and modified with $MgCl_2$.

results mentioned above, it can be concluded that presoaking can enhance Cd adsorption by the biochars by improving hydraulic property and increasing the interaction of internal surfaces of biochar with Cd solution.

4. Conclusions

In this study, the effect of presoaking on Cd adsorption was performed over a range of pH, temperature, and biochar particle size. According to the obtained results, presoaking biochars had a significant effect on Cd adsorption by non-modified or modified rice husk biochars. This effect was also decreased with increasing contact time. The optimum conditions for Cd adsorption by biochars included pH 6, temperature 35 °C, and particle size 100 μm. However, presoaking provided conditions where optimal Cd adsorption was achieved at a lower pH and temperature in the coarser size (500 μm) biochar. It was also found that presoaking, by reducing the micropores of biochar, enhanced biochar contact with the external solution, and presoaked biochars could reach the equilibrium at shorter time. The presoaking effect was more evident at lower temperatures in the biochars with coarser particles. With

Table 4
Data of kinetics model fitting for Cd adsorption in modified and non-modified rice husk biochars.

Biochar type	Presoaking status	Pseudo first order			Pseudo second order			Intraparticle diffusion		
		q_e (mg g^{-1})	k_1 (h^{-1})	R^2	q_e (mg g^{-1})	k_2 ($mg^{-1}g^{-1}h^{-1}$)	R^2	q_e (mg g^{-1})	K_d	R^2
B1	NP	7.37	0.115	0.98	7.289	0.132	0.99	8.09	0.71	0.91
	P	7.56	0.171	0.99	7.65	0.129	0.99	8.51	0.577	0.75
B2	NP	7.11	0.167	0.91	7.11	0.135	0.99	7.95	0.729	0.91
	P	7.52	0.182	0.99	7.52	0.131	0.99	8.34	0.555	0.77
MB1	NP	94.01	0.235	0.99	94.82	0.01	0.99	108.5	9.39	0.77
	P	97.7	0.252	0.98	97.16	0.01	0.99	109.6	7.66	0.73
MB2	NP	94.35	0.184	0.98	95.35	0.101	0.99	111.6	11.42	0.78
	P	98.45	0.196	0.98	98.42	0.009	0.99	113.4	10.75	0.76

P, presoaked biochar; NP, non-presoaked biochar; B1, biochar produced at 450 °C; B2, biochar produced at 600 °C, MB1, biochar produced at 450 °C and modified with MgCl2; and MB2, biochar produced at 600 °C and modified with MgCl2.

decreasing the particle size in biochars and increasing temperature, the effect of presoaking also decreased. Because increasing temperature requires energy, it is also more difficult to separate fine-sized biochars from aqueous media. Accordingly, presoaking biochar prior to use appears to be an effective way to increase the adsorption of heavy metals (e.g., Cd) by modified or unmodified biochars and reduce the time to reach equilibrium, making the heavy metal adsorption process more efficient.

CRediT authorship contribution statement

Bahram Abolfazli Behrooz: Conceptualization, Data curation, Formal analysis, Investigation, Methodology, Writing – original draft. **Shahin Ostan:** Methodology, Supervision, Funding acquisition, Writing – review & editing. **Hossein Mirseyed Hosseini:** Methodology, Supervision, Funding acquisition, Writing – review & editing. **Hasan Etesami:** Methodology, Supervision; Funding acquisition, Writing – review & editing. **Elio Padoan:** Methodology, Supervision, Investigation, Writing – review & editing. **Giuliana Magnacca:** Methodology, Formal analysis, Writing – review & editing. **Franco Ajmone Marsan:** Methodology, Funding acquisition, Writing – review & editing.

Declaration of Competing Interest

The authors declare that they have no known competing financial interests or personal relationships that could have appeared to influence the work reported in this paper.

Data Availability

Data will be made available on request.

Acknowledgments

The authors would like to appreciate the Department of Soil Science at the University of Tehran for supporting this project. The authors also thank the technical staff Agricultural Chemistry and pedology unit in the Department of agronomy and food science of the University of Turin, Italy for providing the instrumentation required for biochar and cadmium analysis and also the staff of the Agricultural Chemistry and pedology unit of the University of Turin (Italy) for their help and support. The Authors also appreciate Dr. Mostafa Marzi and Dr. Mohammad-Hossein Mohammadi for their useful suggestions.

Appendix A. Supporting information

Supplementary data associated with this article can be found in the online version at doi:10.1016/j.ecoenv.2023.114932.

References

Agarwal, M., Singh, K., 2017. Heavy metal removal from wastewater using various adsorbents: a review. J. Water Reuse Desalin. 7, 387–419.
Ai, T., Wu, S., Zhang, R., Gao, M., Zhou, J., Xie, J., Ren, L., Zhang, Z., 2021. Changes in the structure and mechanical properties of a typical coal induced by water immersion. Int. J. Rock. Mech. Min. Sci. 138, 104597.
Akram, A., Muzammal, S., Shakoor, M.B., Ahmad, S.R., Jilani, A., Iqbal, J., Al-Sehemi, A. G., Kalam, A., Aboushoushah, S.F.O., 2022. Synthesis and application of egg shell biochar for As (V) removal from aqueous solutions. Catal 12, 431.
Angın, D., 2013. Effect of pyrolysis temperature and heating rate on biochar obtained from pyrolysis of safflower seed press cake. Bioresour. Technol. 128, 593–597.
Arán, D., Antelo, J., Fiol, S., Macias, F., 2016. Influence of feedstock on the copper removal capacity of waste-derived biochars. Bioresour. Technol. 212, 199–206.
Berslin, D., Reshmi, A., Sivaprakash, B., Rajamohan, N., Kumar, P.S., 2021. Remediation of emerging metal pollutants using environment friendly biochar-Review on applications and mechanism. Chemosphere, 133384.
Brown, T.L., LeMay, H.E., Bursten, B.E., Murphy, C.J., Woodward, P.M., Stoltzfus, M.W., Lufaso, M.W., 2018. Study guide. Chemistry: the central science, 14th ed ed.,. Pearson,.
Chatterjee, R., Sajjadi, B., Chen, W.-Y., Mattern, D.L., Hammer, N., Raman, V., Dorris, A., 2020. Effect of pyrolysis temperature on physicochemical properties and acoustic-based amination of biochar for efficient CO_2 adsorption. Front Energy Res 8, 85.
Chen, T., Zhang, Y., Wang, H., Lu, W., Zhou, Z., Zhang, Y., Ren, L., 2014. Influence of pyrolysis temperature on characteristics and heavy metal adsorptive performance of biochar derived from municipal sewage sludge. Bioresour. Technol. 164, 47–54.
Chen, T., Luo, L., Deng, S., Shi, G., Zhang, S., Zhang, Y., Deng, O., Wang, L., Zhang, J., Wei, L., 2018. Sorption of tetracycline on H3PO4 modified biochar derived from rice straw and swine manure. Bioresour. Technol. 267, 431–437.
Creamer, A.E., Gao, B., Zimmerman, A., Harris, W., 2018. Biomass-facilitated production of activated magnesium oxide nanoparticles with extraordinary CO_2 capture capacity. Chem. Eng. J. 334, 81–88.
Deng, Y., Li, X., Ni, F., Liu, Q., Yang, Y., Wang, M., Ao, T., Chen, W., 2021. Synthesis of magnesium modified biochar for removing copper, lead and cadmium in single and binary systems from aqueous solutions: adsorption mechanism. Water 13, 599.
Ding, Z., Hu, X., Wan, Y., Wang, S., Gao, B., 2016. Removal of lead, copper, cadmium, zinc, and nickel from aqueous solutions by alkali-modified biochar: batch and column tests. J. Ind. Eng. Chem. 33, 239–245.
Faria, P., Orfao, J., Pereira, M., 2004. Adsorption of anionic and cationic dyes on activated carbons with different surface chemistries. Water Res 38, 2043–2052.
Fulazzaky, M.A., 2011. Determining the resistance of mass transfer for adsorption of the surfactants onto granular activated carbons from hydrodynamic column. Chem. Eng. J. 166, 832–840.
Gao, L.-Y., Deng, J.-H., Huang, G.-F., Li, K., Cai, K.-Z., Liu, Y., Huang, F., 2019. Relative distribution of Cd2+ adsorption mechanisms on biochars derived from rice straw and sewage sludge. Bioresour. Technol. 272, 114–122.
Gray, M., Johnson, M.G., Dragila, M.I., Kleber, M., 2014. Water uptake in biochars: The roles of porosity and hydrophobicity. Biomass-.-. Bioenergy 61, 196–205.
Ho, Y.-S., McKay, G., 1999. Pseudo-second order model for sorption processes. Process Biochem 34, 451–465.
Huang, F., Zhang, S.-M., Wu, R.-R., Zhang, L., Wang, P., Xiao, R.-B., 2021. Magnetic biochars have lower adsorption but higher separation effectiveness for Cd2+ from aqueous solution compared to nonmagnetic biochars. Environ. Pollut. 275, 116485.
Ifthikar, J., Wang, J., Wang, Q., Wang, T., Wang, H., Khan, A., Jawad, A., Sun, T., Jiao, X., Chen, Z., 2017. Highly efficient lead distribution by magnetic sewage sludge biochar: sorption mechanisms and bench applications. Bioresour. Technol. 238, 399–406.
Jabro, J.D., Stevens, W.B., 2022. Pore size distribution derived from soil–water retention characteristic curve as affected by tillage intensity. Water 14, 3517.
Jiang, J., Xu, R.-k, Jiang, T.-y, Li, Z., 2012. Immobilization of Cu (II), Pb (II) and Cd (II) by the addition of rice straw derived biochar to a simulated polluted Ultisol. J. Hazard. Mater. 229, 145–150.
Jin, Z., Xiao, S., Dong, H., Xiao, J., Tian, R., Chen, J., Li, Y., Li, L., 2022. Adsorption and catalytic degradation of organic contaminants by biochar: overlooked role of biochar's particle size. J. Hazard. Mater. 422, 126928.

Joseph, L., Jun, B.-M., Flora, J.R., Park, C.M., Yoon, Y., 2019. Removal of heavy metals from water sources in the developing world using low-cost materials: a review. Chemosphere 229, 142–159.
Khan, Z.H., Gao, M., Qiu, W., Islam, M.S., Song, Z., 2020. Mechanisms for cadmium adsorption by magnetic biochar composites in an aqueous solution. Chemosphere 246, 125701.
Kinney, T., Masiello, C., Dugan, B., Hockaday, W., Dean, M., Zygourakis, K., Barnes, R., 2012. Hydrologic properties of biochars produced at different temperatures. Biomass Bioenergy 41, 34–43.
Kloss, S., Zehetner, F., Dellantonio, A., Hamid, R., Ottner, F., Liedtke, V., Schwanninger, M., Gerzabek, M.H., Soja, G., 2012. Characterization of slow pyrolysis biochars: effects of feedstocks and pyrolysis temperature on biochar properties. J. Environ. Qual. 41, 990–1000.
Kołodyńska, D., Wnętrzak, R., Leahy, J., Hayes, M., Kwapiński, W., Hubicki, Z., 2012. Kinetic and adsorptive characterization of biochar in metal ions removal. Chem. Eng. J. 197, 295–305.
Kumar, S., Islam, A.R.M.T., Islam, H.T., Hasanuzzaman, M., Ongoma, V., Khan, R., Mallick, J., 2021. Water resources pollution associated with risks of heavy metals from Vatukoula Goldmine region, Fiji. J. Environ. Manag. 293, 112868.
Lagergren S, K, 1898. About the theory of so-called adsorption of soluble substances. Sven. Vetensk. Handingarl 24, 1–39.
Li, B., Yang, L., Wang, C.-q, Zhang, Q.-p, Liu, Q.-c, Li, Y.-d, Xiao, R., 2017. Adsorption of Cd (II) from aqueous solutions by rape straw biochar derived from different modification processes. Chemosphere 175, 332–340.
Liu, L., Fan, S., 2018. Removal of cadmium in aqueous solution using wheat straw biochar: effect of minerals and mechanism. Environ. Sci. Pollut. Res 25, 8688–8700.
Lucaci, A.R., Bulgariu, D., Ahmad, I., Lisă, G., Mocanu, A.M., Bulgariu, L., 2019. Potential use of biochar from various waste biomass as biosorbent in Co(II) removal processes. Water.
Naeem, M.A., Imran, M., Amjad, M., Abbas, G., Tahir, M., Murtaza, B., Zakir, A., Shahid, M., Bulgariu, L., Ahmad, I., 2019. Batch and column scale removal of cadmium from water using raw and acid activated wheat straw biochar. Water 11, 1438.
Nguyen, T.-B., Truong, Q.-M., Chen, C.-W., Doong, R.-a, Chen, W.-H., Dong, C.-D., 2022. Mesoporous and adsorption behavior of algal biochar prepared via sequential hydrothermal carbonization and ZnCl2 activation. Bioresour. Technol. 346, 126351.
Nimmo, J.R., 2004. Porosity and pore size distribution. Encycl. Soils Environ. 3, 295–303.
Nnadozie, E.C., Ajibade, P.A., 2020. Adsorption, kinetic and mechanistic studies of Pb (II) and Cr (VI) ions using APTES functionalized magnetic biochar. Microporous Mesoporous Mater. 309, 110573.
Park, C.M., Han, J., Chu, K.H., Al-Hamadani, Y.A., Her, N., Heo, J., Yoon, Y., 2017. Influence of solution pH, ionic strength, and humic acid on cadmium adsorption onto activated biochar: experiment and modeling. J. Ind. Eng. Chem. 48, 186–193.
Qiu, B., Tao, X., Wang, H., Li, W., Ding, X., Chu, H., 2021. Biochar as a low-cost adsorbent for aqueous heavy metal removal: a review. J. Anal. Appl. Pyrolysis 155, 105081.
Quan, G., Fan, Q., Sun, J., Cui, L., Wang, H., Gao, B., Yan, J., 2020. Characteristics of organo-mineral complexes in contaminated soils with long-term biochar application. J. Hazard. Mater. 384, 121265.
Rajapaksha, A.U., Chen, S.S., Tsang, D.C.W., Zhang, M., Vithanage, M., Mandal, S., Gao, B., Bolan, N.S., Ok, Y.S., 2016. Engineered/designer biochar for contaminant removal/immobilization from soil and water: potential and implication of biochar modification. Chemosphere 148, 276–291.
Rasa, K., Heikkinen, J., Hannula, M., Arstila, K., Kulju, S., Hyväluoma, J., 2018. How and why does willow biochar increase a clay soil water retention capacity? Biomass Bioenergy 119, 346–353.
Saha, R., Tripathi, R., 1979. Effect of temperature on hydraulic conductivity of soil. J. Indian Soci. Soil Sci. 27, 220–224.
Sheela, T., Nayaka, Y.A., 2012. Kinetics and thermodynamics of cadmium and lead ions adsorption on NiO nanoparticles. Chem. Eng. J. 191, 123–131.
Shen, Z., Hou, D., Jin, F., Shi, J., Fan, X., Tsang, D.C., Alessi, D.S., 2019. Effect of production temperature on lead removal mechanisms by rice straw biochars. Sci. Total Environ. 655, 751–758.
Shi, J., Fan, X., Tsang, D.C., Wang, F., Shen, Z., Hou, D., Alessi, D.S., 2019. Removal of lead by rice husk biochars produced at different temperatures and implications for their environmental utilizations. Chemosphere 235, 825–831.
Singh, B., Camps-Arbestain, M., Lehmann, J., 2017. Biochar: A Guide to Analytical Methods. Csiro Publishing.
Soedarmanto, H., Sudjito, Wijayanti, W., Hamidi, N., Setiawati, E., 2020. The impact of water soaking on physicochemical activated carbon produced by various thermal cracking temperature. AIP Conference Proceedings. AIP Publishing LLC, 020008.
Song, B., Chen, M., Zhao, L., Qiu, H., Cao, X., 2019. Physicochemical property and colloidal stability of micron-and nano-particle biochar derived from a variety of feedstock sources. Sci. Total Environ. 661, 685–695.
Srivastava, V.C., Swamy, M.M., Mall, I.D., Prasad, B., Mishra, I.M., 2006. Adsorptive removal of phenol by bagasse fly ash and activated carbon: equilibrium, kinetics and thermodynamics. Colloids Surf. a: Physicochem. Eng. Asp. 272, 89–104.
Srivastava, V.C., Mall, I.D., Mishra, I.M., 2007. Adsorption thermodynamics and isosteric heat of adsorption of toxic metal ions onto bagasse fly ash (BFA) and rice husk ash (RHA). Chem. Eng. J. 132, 267–278.
Sun, C., Chen, T., Huang, Q., Wang, J., Lu, S., Yan, J., 2019. Enhanced adsorption for Pb (II) and Cd (II) of magnetic rice husk biochar by KMnO 4 modification. Environ. Sci. Pollut. Res 26, 8902–8913.
Tan, X.-f, Liu, Y.-g, Gu, Y.-l, Xu, Y., Zeng, G.-m, Hu, X.-j, Liu, S.-b, Wang, X., Liu, S.-m, Li, J., 2016. Biochar-based nano-composites for the decontamination of wastewater: A review. Bioresour. Technol. 212, 318–333.
Teng, D., Zhang, B., Xu, G., Wang, B., Mao, K., Wang, J., Sun, J., Feng, X., Yang, Z., Zhang, H., 2020. Efficient removal of Cd (II) from aqueous solution by pinecone biochar: sorption performance and governing mechanisms. Environ. Pollut. 265, 115001.
Usman, A., Sallam, A., Zhang, M., Vithanage, M., Ahmad, M., Al-Farraj, A., Ok, Y.S., Abduljabbar, A., Al-Wabel, M., 2016. Sorption process of date palm biochar for aqueous Cd (II) removal: efficiency and mechanisms. Water Air Soil Pollut. 227, 1–16.
Van't, Hoff, J., 1888. XII. The function of osmotic pressure in the analogy between solutions and gases. Lond., Edinb., Dublin Philos. Mag. J. Sci. 26, 81–105.
Vogel, H.-J., Roth, K., 2001. Quantitative morphology and network representation of soil pore structure. Adv. Water Resour. 24, 233–242.
Wang, D., Luo, W., Zhu, J., Wang, T., Gong, Z., Fan, M., 2021. Potential of removing Pb, Cd, and Cu from aqueous solutions using a novel modified ginkgo leaves biochar by simply one-step pyrolysis. Biomass Convers. Biorefin 1–10.
Wang, H., Wang, X., Ma, J., Xia, P., Zhao, J., 2017. Removal of cadmium (II) from aqueous solution: a comparative study of raw attapulgite clay and a reusable waste–struvite/attapulgite obtained from nutrient-rich wastewater. J. Hazard. Mater. 329, 66–76.
Wang, L., Wang, Y., Ma, F., Tankpa, V., Bai, S., Guo, X., Wang, X., 2019. Mechanisms and reutilization of modified biochar used for removal of heavy metals from wastewater: a review. Sci. Total Environ. 668, 1298–1309.
Wang, W., Kang, R., Yin, Y., Tu, S., Ye, L., 2022. Two-step pyrolysis biochar derived from agro-waste for antibiotics removal: Mechanisms and stability. Chemosphere 292, 133454.
Weber Jr, W.J., Morris, J.C., 1963. Kinetics of adsorption on carbon from solution. J. Sanit. Eng. Div. 89, 31–59.
Wen, J., Xue, Z., Yin, X., Wang, X., 2022. Insights into aqueous reduction of Cr (VI) by biochar and its iron-modified counterpart in the presence of organic acids. Chemosphere 286, 131918.
Wu, J., Wang, T., Wang, J., Zhang, Y., Pan, W.-P., 2021. A novel modified method for the efficient removal of Pb and Cd from wastewater by biochar: Enhanced the ion exchange and precipitation capacity. Sci. Total Environ. 754, 142150.
Xiang, J., Lin, Q., Cheng, S., Guo, J., Yao, X., Liu, Q., Yin, G., Liu, D., 2018. Enhanced adsorption of Cd (II) from aqueous solution by a magnesium oxide–rice husk biochar composite. Environ. Sci. Pollut. Res 25, 14032–14042.
Xiao, Y., Xue, Y., Gao, F., Mosa, A., 2017. Sorption of heavy metal ions onto crayfish shell biochar: effect of pyrolysis temperature, pH and ionic strength. J. Taiwan Inst. Chem. Eng. 80, 114–121.
Xu, X., Hu, X., Ding, Z., Chen, Y., Gao, B., 2017. Waste-art-paper biochar as an effective sorbent for recovery of aqueous Pb (II) into value-added PbO nanoparticles. Chem. Eng. J. 308, 863–871.
Yadav, M., Singh, G., Jadeja, R., 2021. Physical and chemical methods for heavy metal removal. Pollut. Water Manag. Resourc. Strateg. Scarcity 377–397.
Yang, G., Xu, Y., Huo, L., Wang, H., Guo, D., 2022. Analysis of temperature effect on saturated hydraulic conductivity of the chinese loess. Water 14, 1327.
Yi, X., Zhang, S., Bai, Z., Deng, J., Shu, C., Qu, G., Ge, L., 2022. Effect of water soaking on the microstructure and spontaneous combustion characteristics of Bituminous coal during Low− temperature oxidation. Combust. Sci. Technol. 1–25.
Yin, G., Tao, L., Chen, X., Bolan, N.S., Sarkar, B., Lin, Q., Wang, H., 2021. Quantitative analysis on the mechanism of Cd2+ removal by MgCl2-modified biochar in aqueous solutions. J. Hazard. Mater. 420, 126487.
Zhai, X., Ge, H., Wang, T., Shu, C.-M., Li, J., 2020. Effect of water immersion on active functional groups and characteristic temperatures of bituminous coal. Energy 205, 118076.
Zhang, D., Zhang, K., Hu, X., He, Q., Yan, J., Xue, Y., 2021. Cadmium removal by $MgCl_2$ modified biochar derived from crayfish shell waste: Batch adsorption, response surface analysis and fixed bed filtration. J. Hazard. Mater. 408, 124860.
Zhang, J., Liu, J., Liu, R., 2015. Effects of pyrolysis temperature and heating time on biochar obtained from the pyrolysis of straw and lignosulfonate. Bioresour. Technol. 176, 288–291.
Zhou, Y., Gao, B., Zimmerman, A.R., Chen, H., Zhang, M., Cao, X., 2014. Biochar-supported zerovalent iron for removal of various contaminants from aqueous solutions. Bioresour. Technol. 152, 538–542.